



## The Exceptional 2018 European Water Seesaw Calls for Action on Adaptation

Andrea Toreti, Alan Belward, Ignacio Perez-dominguez, Gustavo Naumann, Jürg Luterbacher, Ottmar Cronie, Lorenzo Seguni, Giacinto Manfron, Raul Lopez-Lozano, Bettina Baruth, et al.

### ► To cite this version:

Andrea Toreti, Alan Belward, Ignacio Perez-dominguez, Gustavo Naumann, Jürg Luterbacher, et al.. The Exceptional 2018 European Water Seesaw Calls for Action on Adaptation. *Earth's Future*, 2019, 12 p. 10.1029/2019EF001170 . hal-02629352

**HAL Id: hal-02629352**

**<https://hal.inrae.fr/hal-02629352>**

Submitted on 27 May 2020

**HAL** is a multi-disciplinary open access archive for the deposit and dissemination of scientific research documents, whether they are published or not. The documents may come from teaching and research institutions in France or abroad, or from public or private research centers.

L'archive ouverte pluridisciplinaire **HAL**, est destinée au dépôt et à la diffusion de documents scientifiques de niveau recherche, publiés ou non, émanant des établissements d'enseignement et de recherche français ou étrangers, des laboratoires publics ou privés.

## Earth's Future



## RESEARCH ARTICLE

10.1029/2019EF001170

## Key Points:

- Unique concurrent spring and summer climatic anomalies affected Europe in 2018
- 2018-like droughts could become a common occurrence as early as 2043
- Climate change adaptation strategies for agriculture in Europe cannot count on recurrent water seesaws

## Supporting Information:

- Supporting Information S1

## Correspondence to:

A. Toreti,  
andrea.toreti@ec.europa.eu

## Citation:

Toreti, A., Belward, A., Perez-Dominguez, I., Naumann, G., Luterbacher, J., Cronie, O., et al. (2019). The exceptional 2018 European water seesaw calls for action on adaptation. *Earth's Future*, 7. <https://doi.org/10.1029/2019EF001170>

Received 29 JAN 2019

Accepted 7 MAY 2019

Accepted article online 15 MAY 2019

## The Exceptional 2018 European Water Seesaw Calls for Action on Adaptation

Andrea Toreti<sup>1</sup> , Alan Belward<sup>1</sup>, Ignacio Perez-Dominguez<sup>2</sup> , Gustavo Naumann<sup>1</sup> , Jürg Luterbacher<sup>3</sup> , Ottmar Cronie<sup>4</sup> , Lorenzo Seguíni<sup>1</sup>, Giacinto Manfron<sup>1</sup> , Raul Lopez-Lozano<sup>1</sup> , Bettina Baruth<sup>1</sup>, Maurits van den Berg<sup>1</sup>, Frank Dentener<sup>1</sup> , Andrej Ceglar<sup>1</sup> , Thomas Chatzopoulos<sup>2</sup>, and Matteo Zampieri<sup>1</sup>

<sup>1</sup>European Commission, Joint Research Centre (JRC), Ispra, Italy, <sup>2</sup>European Commission, Joint Research Centre (JRC), Seville, Spain, <sup>3</sup>Department of Geography, Climatology, Climate Dynamics and Climate Change, Centre for International Development and Environmental Research, Justus-Liebig University of Giessen, Giessen, Germany, <sup>4</sup>Department of Mathematics and Mathematical Statistics, Umeå University, Umeå, Sweden

**Abstract** Temperature and precipitation are the most important factors responsible for agricultural productivity variations. In 2018 spring/summer growing season, Europe experienced concurrent anomalies of both. Drought conditions in central and northern Europe caused yield reductions up to 50% for the main crops, yet wet conditions in southern Europe saw yield gains up to 34%, both with respect to the previous 5-year mean. Based on the analysis of documentary and natural proxy-based seasonal paleoclimate reconstructions for the past half millennium, we show that the 2018 combination of climatic anomalies in Europe was unique. The water seesaw, a marked dipole of negative water anomalies in central Europe and positive ones in southern Europe, distinguished 2018 from the five previous similar droughts since 1976. Model simulations reproduce the 2018 European water seesaw in only 4 years out of 875 years in historical runs and projections. Future projections under the RCP8.5 scenario show that 2018-like temperature and rainfall conditions, favorable to crop growth, will occur less frequent in southern Europe. In contrast, in central Europe high-end emission scenario climate projections show that droughts as intense as 2018 could become a common occurrence as early as 2043. While integrated European and global agricultural markets limited agro-economic shocks caused by 2018's extremes, there is an urgent need for adaptation strategies for European agriculture to consider futures without the benefits of any water seesaw.

## 1. Introduction

Climate change poses particular challenges for agricultural production systems as plant growth is affected by climate conditions (e.g., Gray & Brady, 2016; Lobell & Gourdji, 2012; Porter & Semenov, 2005). Rising temperatures, changes in precipitation regimes, and increasing frequency, duration, and intensity of extreme events negatively affect crop yields and fodder production (e.g., Asseng et al., 2014; Toreti, Bassu, et al., 2019; Webber et al., 2018; Zhao et al., 2017). The adverse impacts of climate extremes on the main crops in the last decades have been addressed in numerous studies (e.g., Deryng et al., 2014; Fontana et al., 2015; Lesk et al., 2016; Rezaei, Siebert, Manderscheid, et al., 2018; Zampieri et al., 2017). Besides heat stress, drought and water excess have been shown to trigger losses when occurring in critical phenological phases. Thus, to reduce the impacts associated with these extreme events at the local scale, agricultural management and planning need to consider them in the development and implementation of risk reduction strategies.

At the regional scale, the push/pull of droughts in one region and the absence of water stress elsewhere (i.e., the water seesaw) can translate into crop yield differentials. Thus, it is key to estimate how often water seesaw conditions have occurred and will occur and to understand if climate change adaptation strategies for agriculture can count on recurrent water seesaws. The extreme climate conditions experienced by Europe in 2018 have triggered all these questions.

## 2. Data and Methods

Starting from the 2018 event as a reference, we investigate past, current, and future water seesaw events. The following data sets are used to perform such analysis: daily climate observations from ground weather

©2019. The Authors.  
This is an open access article under the terms of the Creative Commons Attribution-NonCommercial-NoDerivs License, which permits use and distribution in any medium, provided the original work is properly cited, the use is non-commercial and no modifications or adaptations are made.

stations covering the last decades from 1976, remote sensing data, atmospheric reanalysis, paleoclimate reconstructions covering the last ~500 years, and climate projections till 2100. The observational climate gridded data set (MarsMet) used is maintained by the Joint Research Centre of the European Commission (Toreti, Maiorano, et al., 2019). This data set covers the European Union and its neighboring countries at a spatial resolution of 25 km.

The remote sensing analysis of vegetation status is based on the fraction of absorbed photosynthetically active radiation data (fAPAR; an indicator related to biomass; Verger et al., 2014) obtained from the Copernicus Global Land Service, more specifically, the fAPAR version 2 at 1 km (Verger et al., 2014).

The large-scale atmospheric circulation during the spring-to-summer period is analyzed by using geopotential height values at 500 hPa from the ERA-Interim reanalysis (Dee et al., 2011).

Gridded multiproxy, documentary and natural proxy-based paleoclimate reconstructions of seasonal temperature (Luterbacher et al., 2004) and precipitation (Pauling et al., 2006) covering the period back to 1500 CE are also used. The climate model projections under the high-end emission scenario RCP8.5 come from the FP7-project HELIX (High-End cLimate Impacts and eXtremes; www.helixclimate.eu). They have been obtained with the atmospheric model EC-EARTH3-HR v3.1 (Hazeleger et al., 2012) at 0.35° (with an improved dynamics and parameterization) having prescribed Sea Surface Temperature and Sea Ice concentration originating from seven independent CMIP5 GCMs (see Table S1 in the supporting information and Naumann et al., 2018). The higher spatial resolution, compared to CMIP5 model runs, can positively affect the representation of the hydrological cycle and the atmospheric blocking condition (Berckmans et al., 2013; Dawson & Palmer, 2015; Wyser et al., 2017).

The 2018 drought affected central and northern Europe; however, in this study we focus only on central Europe being the geographic core of the event and to facilitate the spatial analysis and comparison with the other observed, reconstructed, and projected drought events. Central Europe is here defined as the region spanning the following latitude/longitude limits: 3–20° E, 46–56° N. While southern Europe is defined by 10° W–30° E, 36.5–45.5° N.

The water seesaw is characterized by using the Standardized Precipitation Evapotranspiration Index (SPEI; Vicente-Serrano et al., 2010) computed by using precipitation data and the FAO-recommended Penmann-Monteith evapotranspiration function (Allen et al., 1998). Furthermore, these anomalous climate conditions are also characterized and analyzed by studying concurrent seasonal (spring and summer) temperature and precipitation extremes.

The spatial distributions of the temperature and precipitation quantiles, as well as of the SPEI values, are compared with the ones in 2018 by using the Kullback-Leibler (KL) divergence. Given distributions  $P$  and  $Q$  to be compared, which have probability densities  $p$  and  $q$ , respectively, the KL divergence is defined as

$$D(P||Q) = \int p(x) \log \frac{p(x)}{q(x)} dx. \quad (1)$$

Here  $Q$  is for instance the spatial distribution of the 2018 SPEI values in central Europe, while  $P$  is the spatial distribution of the SPEI values of any other year to be compared with 2018. Given observations  $x_1, \dots, x_n$ , we here estimate the KL divergence by means of (Perez-Cruz, 2008):

$$\hat{D}(P||Q) = -1 + \frac{1}{n} \sum_{i=1}^n \log \frac{\Delta P_c(x_i)}{\Delta Q_c(x_i)}, \quad (2)$$

where  $\Delta P_c(x_i) = P_c(x_i) - P_c(x_i - \epsilon)$  for any  $\epsilon < \min_i \{x_i - x_{i-1}\}$  and  $P_c$  is the continuous piecewise extension of the stepwise empirical cumulative distribution function.

The spatiotemporal intensity functions of the drought events and the anomalous wet conditions are estimated with a resample-smoothed Voronoi estimator (Moradi et al., 2019). Let  $Y = \{x_1, \dots, x_N\} \subset [0, T]$  be the collection of random time points associated to the events occurring in the time interval  $[0, T]$ , and denoting the associated spatial extents with  $\underline{s} \leq s_i \leq \bar{s}$ ,  $i = 1, \dots, N$ , we obtain the spatiotemporal point process  $X = \{(x_1, s_1), \dots, (x_N, s_N)\} \subset [0, T] \times [\underline{s}, \bar{s}]$ . Let further  $X_{1,p}, \dots, X_{m,p}$  be  $m \geq 1$  independent  $p$ -thinnings of  $X$ ,  $0 \leq p \leq 1$ ; we obtain each collection  $X_{i,p}$  by running through the points of  $X$  and independently

Comment citer ce document :

throwing out each of its points with probability  $1 - p$ . Then, the resample-smoothed Voronoi estimator (Moradi et al., 2019) is given by

$$\hat{\rho}_{p,m}(t, v) = \frac{1}{mp} \sum_{i=1}^m \hat{\rho}_i(t, v) = \sum_{i=1}^m \sum_{(x,s) \in X_{i,p}} \frac{\mathbb{1}\{(t, v) \in \mathcal{V}_{(x,s)}(X_{i,p})\}}{mp |\mathcal{V}_{(x,s)}(X_{i,p})|}, (t, v) \in [0, T] \times [\underline{s}, \bar{s}], \quad (3)$$

where for any  $(x, s) \in X_{i,p}$ ,  $|\mathcal{V}_{(x,s)}(X_{i,p})|$  is the size of

$$\mathcal{V}_{(x,s)}(X_{i,p}) = \{u \in [0, T] \times [\underline{s}, \bar{s}] : \|u - (x, s)\| \leq \|u - (x', s')\| \text{ for any } (x', s') \in X_{i,p} \setminus \{(x, s)\}\}, \quad (4)$$

which is the Voronoi cell consisting of all points  $u \in [0, T] \times [\underline{s}, \bar{s}]$  closer to  $(x, s)$  than any  $(x', s') \in X_{i,p} \setminus \{(x, s)\}$  in terms of the Euclidean distance. It has been suggested (Moradi et al., 2019) to choose  $p$  and  $m$  such that  $0 < p \leq 0.2$  and  $m \geq 400$ . The interval  $[0, T]$  is here chosen empirically by letting 0 represent the first observed event time minus half its distance to the second smallest observed event time.  $T$  is chosen similarly but considering the largest observed event, and this allows to correct for the edge effects/bias (Moradi et al., 2019). The same procedure is applied to the spatial extension.

To identify when the 2018-like drought events will become a common occurrence in the climate projections, we use the intensity function thresholded at 0.5; that is, we identify the year when the estimated intensity function exceeds and remains above 0.5. This implies that in a given year it is more likely to observe an extreme drought event, such as the one in 2018, than not.

### 3. Results

#### 3.1. The 2018 Climate Extreme

In 2018 drought affected central and northern Europe, with an exceptionally negative spring/summer water balance. At its geographic core, this deficit also affected the first months of the year (Figure S1). According to the SPEI, the 2018 drought event can be classified as severe to extreme both at 3-month (June to August) and 6-month (March to August) time scales (Figure 1). In central Europe over 34% of the landmass is used for agriculture, and 52% of the entire region suffered severe-to-extreme drought (SPEI-6 less than  $-1.5$ ; Figure 1), while 20% was affected by extreme drought (SPEI-6 less than  $-2$ ; Figure 1). Meanwhile, southern Europe experienced wetter than usual spring (March to May) conditions, and to a certain extent also summer (June to August), with large areas characterized by SPEI-6 higher than 1.5 and 2 (Figure 1). The exceptional wet conditions in March 2018 over the Iberian Peninsula brought to an end the 2016–2017 drought and were induced by an exceptional planetary wave activity, followed by a sudden stratospheric warming and a subsequent persistent negative North Atlantic Oscillation anomaly (Ayarzagüena et al., 2018).

The 2018 drought was characterized by (i) a relatively dry spring (March, April, and May) with 3-month total precipitation being in the lower percentiles of the 1976–2005 distribution (with the median of central Europe equal to the 40th percentile; Figure S2). (ii) Exceptionally high mean spring temperatures were also recorded, all in the highest percentiles of the 1976–2005 distribution (spatial median greater than the 99th percentile; Figure S2). Finally, (iii) a dry summer (June, July, and August) with total precipitation in the lowest percentiles (i.e., median equal to the 17th percentile) associated with (iv) very warm mean temperatures in the highest percentiles of the 1976–2005 distribution (spatial median equal to the 97th percentile; Figure S2) were observed. This comparison in terms of percentiles based on the 1976–2005 distribution helps to understand and quantify how anomalous the 2018 conditions were in a climatological perspective.

The large-scale atmospheric circulation was characterized by pronounced positive geopotential height anomalies in April (Figure 2), covering a large area centered over eastern Europe and extending to the Mediterranean in the South and to central Europe in the West. These atmospheric conditions persisted in subsequent months and moved northward bridging toward the North Atlantic. In May, the geopotential height anomalies were covering a large area stretching from the Scandinavian Peninsula to the Atlantic. In August, this anomaly moved South and elongated from the North Atlantic to western Russia (Figure 2). The complex evolution of these blocking conditions highlights both the higher intensity of the anomalies and the broader spatial extension (e.g., compared to the classification of Stefanon et al., 2012), which contribute to explain the exceptional observed temperature anomalies. The occurrence and persistence of atmospheric blocking conditions are key factors in the development of large-scale heat wave and drought, and to trigger soil-moisture temperature feedbacks (Brunner et al., 2018, 2017; Miralles et al., 2014; Luterbacher et al., 2004).

Comment citer ce document :

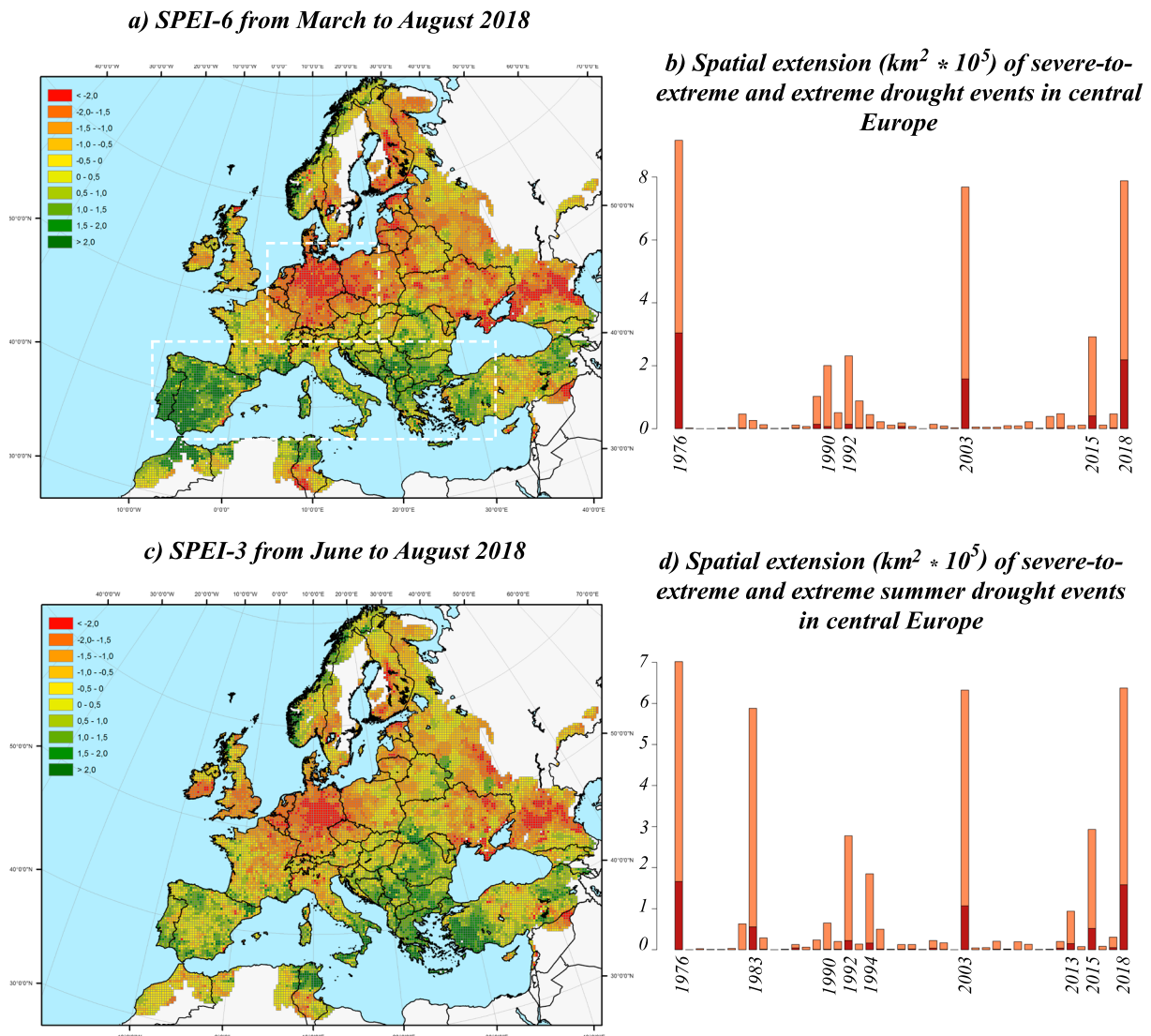


**Figure 1.** (a) 2018 estimated SPEI-6 (March–August) and (b) associated spatial extent ( $\text{km}^2 \cdot 10^5$ ) of the severe-to-extreme (orange bars) and extreme (red bars) drought events in central Europe from 1976 to 2018. The white boxes in (a) indicate the two regions of interest: southern Europe and central Europe. (c) 2018 estimated SPEI-3 (June–August) and associated (d) spatial extent ( $\text{km}^2 \cdot 10^5$ ) of the severe-to-extreme (orange bars) and extreme (red bars) drought events in central Europe from 1976 to 2018. SPEI = Standardized Precipitation Evapotranspiration Index.

The severity of the 2018 drought as well as the pronounced water seesaw can be visualized in the anomalous fAPAR values from March to August (spring and summer) compared with the entire measurement period 1999–2017 (Figure 3). The drought event impacted plant growth in large areas of central and northern Europe and exceptionally reduced biomass accumulation, as suggested by fAPAR anomalies of 15–25% (compared to 1999–2017; Figures 3 and S3 on agricultural areas) even exceeding 25% locally. In these regions, the 2018 summer biomass accumulation in the agricultural areas (as inferred by the fAPAR) was the lowest of the entire observational record since 1999 (Figure 3). In contrast, southern Europe experienced above-normal biomass accumulation (Figure 3) sustained by the exceptional spring precipitation.

### 3.2. The 2018 Extreme Event in a Paleoclimate Perspective

By using the SPEI-6 spatial distribution applied to the available observational records since 1976, only five events resemble the 2018 drought in central Europe: 1976, 1990, 1992, 2003, and 2015 (Figure S4). However, none of these years was characterized by a water seesaw as/as pronounced as the one in 2018. The 2018 drought in central Europe compares well in extent with the drought in 1976 and 2003 (Figures 1 and S4). The 1976 drought has often been considered a benchmark due to its severity (Burke et al., 2010; Briffa et al.,

Comment citer ce document :



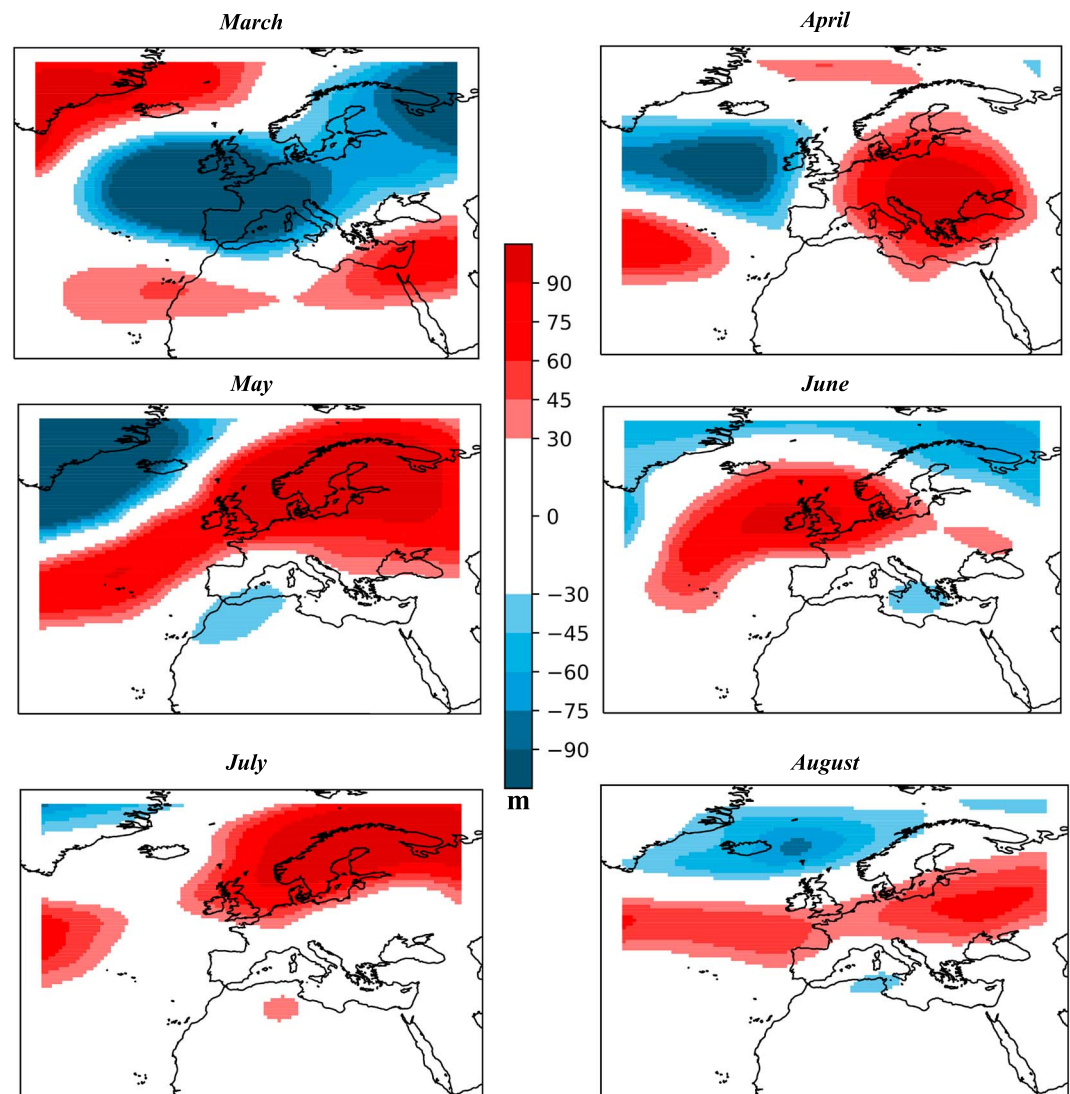


**Figure 2.** Anomalies (with respect to the available data period) of the 2018 monthly (from March to August) geopotential height at 500 hPa as represented by ERA-Interim (values in meters).

2009), with one of the longest heat waves (in the observational records) from June to August and negative rainfall anomalies from May to August. The 2003 event and its impacts have been described and analyzed in several studies (Ciais et al., 2005; Fink et al., 2004; Garcia-Herrera et al., 2010). The 1990 and 1992 droughts were among the biggest events in Europe since 1950 (Spinoni et al., 2015), while the 2015 event in central Europe was even drier in summer than 2003 (Orth et al., 2016b). Concerning the summer heat waves in 1976, 1992, and 2003, the contribution of Mediterranean dry springs was highlighted by Zampieri et al. (2009).

The combination of dry spring, the exceptionally warm spring/summer temperatures, and the dry summer makes the 2018 event unique in a longer climatological perspective. Studying seasonal European temperature and precipitation gridded paleo-reconstructions back to 1500 CE reveals no events similar to 2018 in central Europe in terms of concurrent spring-to-summer temperature and precipitation quantiles spatial distribution (Figure 4). Focusing on summer months alone (June to August), a few events appear to be similar to 2018, notably the 1540 and 1947 droughts. According to reconstructed temperature and precipitation fields, the 1540 event was characterized by a very dry and warm summer (similar to the 2018 one) though spring conditions were even drier than in 2018 (Figure 4). However, though drier, the extreme 2018 spring temperatures were not reached. The 1540 event is also unique from a climate perspective (Orth et al., 2016a; Pfister, 2016; Wetter et al., 2014). In 1540, chronicles narrate of people taking refuge in cellars during the

Comment citer ce document :

Toroti, A. (Auteur de correspondance), Belward, A., PerezDominguez, I., Naumann, G., Luterbacher, J., Cronie, O., Seguin, L., Manfron, G., Lopez-Lozano, R., Baruth, B., Berg, M. v. d., Dentener, F., Ceglar, A., Chatzopoulos, T., Zampieri, M. (2019). The Exceptional 2018 European Water Seesaw Calls for Action on Adaptation. *Earth's Future*, 12 p. . DOI : 10.1029/2019EF001170

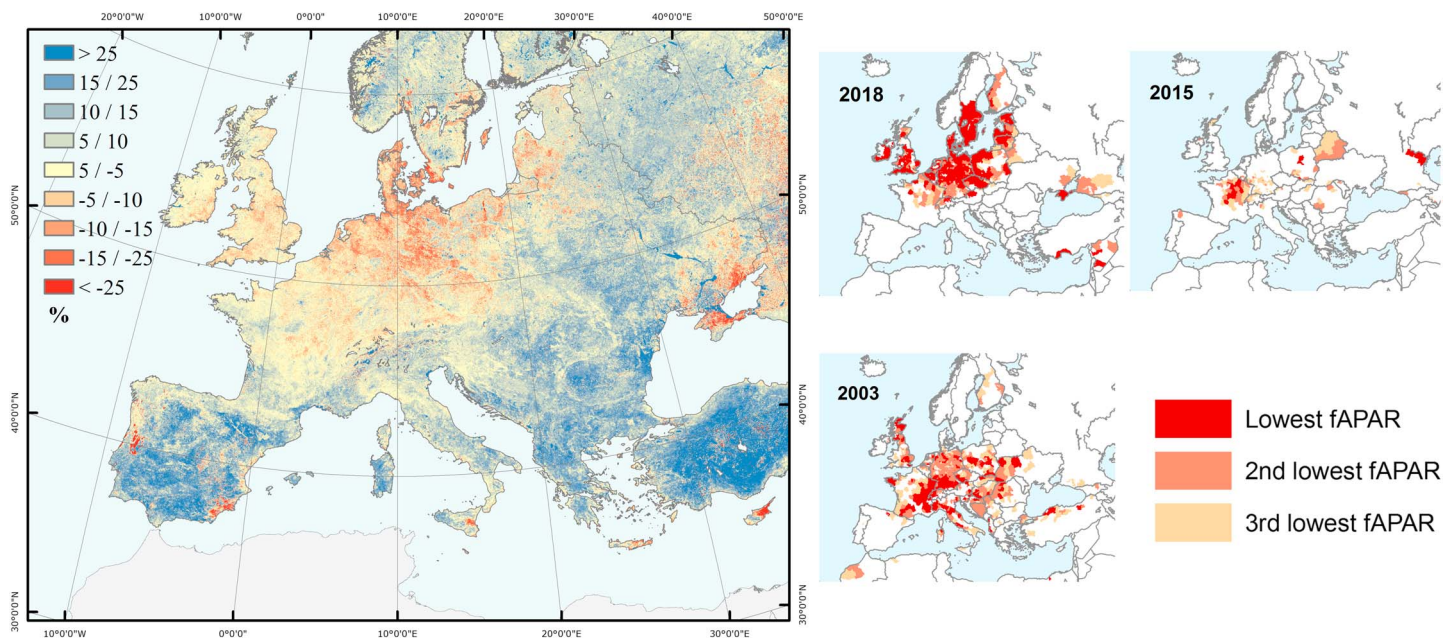


**Figure 3.** (Left panel) Anomalies (percent) of the fAPAR accumulated from March to August 2018 with respect to 1999–2017. (Right panel) Regions where the 2018, 2015, and 2003 summer (June to August) fAPARs (calculated on agricultural land) were the lowest, second lowest, and third lowest since 1999. fAPAR = fraction of absorbed photosynthetically active radiation data.

day in France, of autumn-like trees and forest fires in many areas of Europe (Pfister, 2016), while the entire agricultural sector was heavily affected with cattle dying of thirst and hunger and complete loss of spring grains, legumes, and fruits (Pfister, 2016).

By looking only at the summer temperature conditions being as extreme as the 2018 one (or more), 14 events can be identified since 1500 CE, 5 of them being in the 16th century and 3 in the 20th century and the 2003. While 2018-similar extreme spring conditions are more rare with only five events detected in the last 500 years: 1794, 1822, 1994, 2000, and 2007. This points again to the importance and uniqueness of the concurrent extreme conditions both in spring and summer that characterized the 2018 event. The contribution of the exceptionally and rare warm spring conditions can be evaluated by performing an idealized experiment:

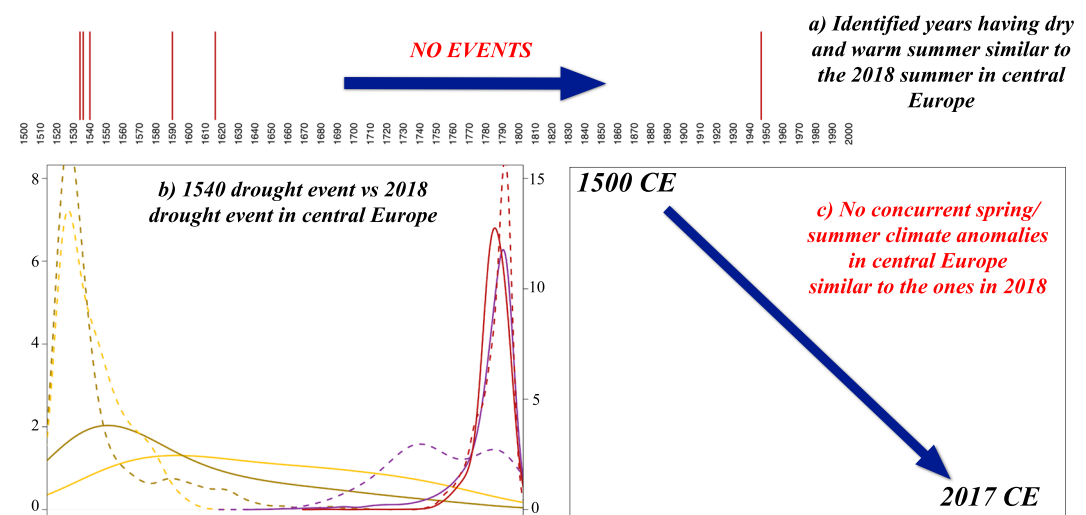


**Figure 4.** (a) 2018-like summer drought events in central Europe identified by using as metric the concurrent spatial distribution of spring and summer temperature and precipitation quantiles. (b) Estimated spatial probability density functions of spring and summer temperatures (red for summer and violet for spring) and precipitation (yellow for spring and brown for summer) in 1540 (dashed lines) and 2018 (bold lines).

Comment citer ce document :

Toroti, A. (Auteur de correspondance), Belward, A., PerezDominguez, I., Naumann, G., Luterbacher, J., Cronie, O., Seguin, L., Manfron, G., Lopez-Lozano, R., Baruth, B., Berg, M. v. d., Dentener, F., Ceglar, A., Chatzopoulos, T., Zampieri, M. (2019). The Exceptional 2018 European Water Seesaw Calls for Action on Adaptation. *Earth's Future*. 12 p. . DOI : 10.1029/2019EF001170

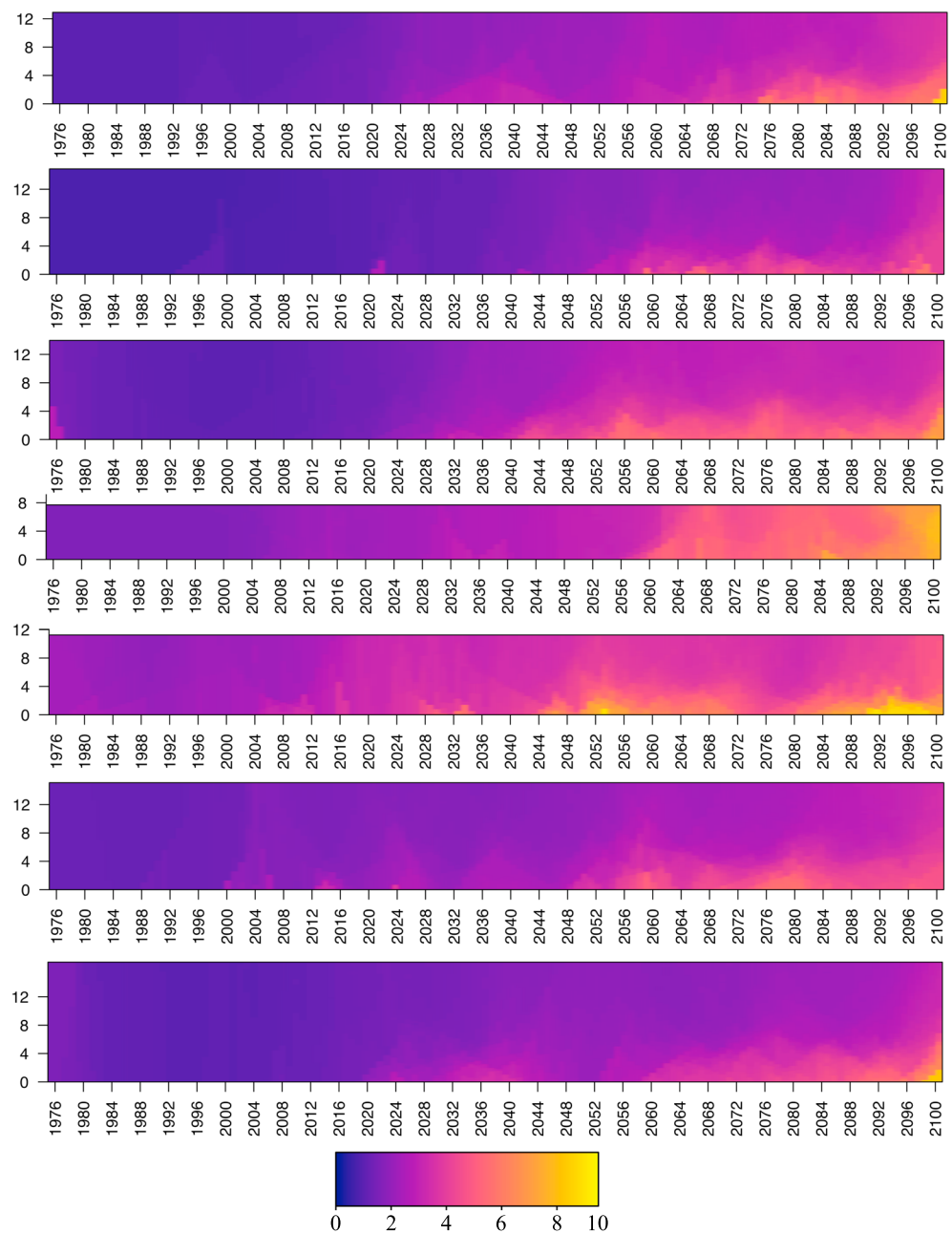


**Figure 5.** Estimated spatiotemporal (time of occurrence in the x axis and spatial extent  $\times 10^5$  in the y axis) frequency of extreme drought events (Standardized Precipitation Evapotranspiration Index-6  $< -2$ ) in central Europe as identified in the seven climate model simulations from 1976 to 2100 under the high-end emission scenario RCP8.5. Values in the frequency legend are  $\times 10^{-2}$ .

the SPEI-6 (from March to August) and its spatial distribution in central Europe are rederived by replacing the extreme spring temperatures with average values, while all the other factors (i.e., drier spring precipitation, very warm, and dry summer) are kept as they were observed in 2018. The spatial distribution of this idealized SPEI still points to severe drought conditions but not to extreme ones (not shown).

### 3.3. Future Projections

To understand how the frequency and severity of the 2018 water seesaw and its drought component might change in the coming decades over Europe, climate projections till 2100 are analyzed. As done for the period covered by observational gridded data (1976–2018), we derive SPEI-3 (June–August) and SPEI-6 (March–August). Then, we investigate their changes and identify events similar to 2018 (i.e., with

Comment citer ce document :



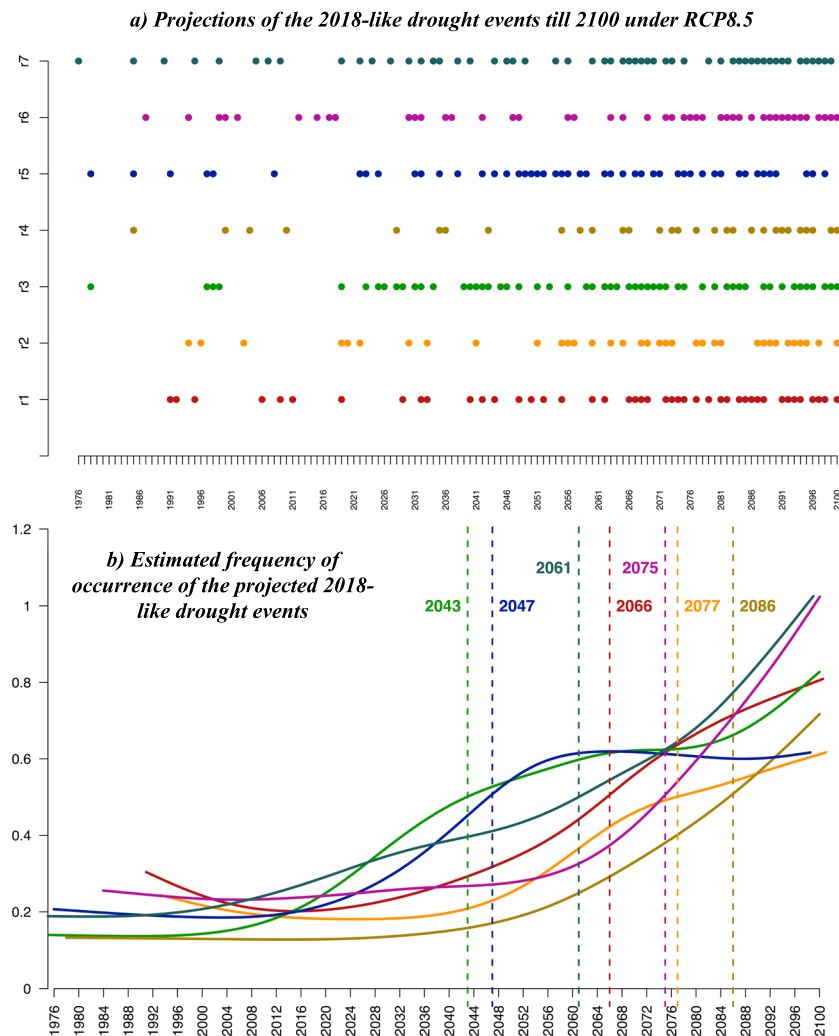


**Figure 6.** (a) 2018-like drought events in central Europe in the seven climate model simulations from 1976 to 2100 under the high-end emission scenario RCP8.5. The events have been identified by using the spatial distribution of the estimated Standardized Precipitation Evapotranspiration Index-6. (b) Estimated frequency of occurrence of the 2018-like drought events in central Europe in the seven climate model simulations from 1976 to 2100. The dashed lines indicate when these events will become the norm in each simulation.

similar spatial distribution of SPEI values). The combined spatiotemporal SPEI analysis (investigating both the occurrence and the spatial extent) of extreme drought events (SPEI less than  $-2$ ) in central Europe reveals an increased frequency toward the end of the century in all seven climate realizations (Figure 5). However, the magnitude of these changes (especially concerning the spatial extent) varies among the seven climate model projections (Figure 5). Similar findings characterize the severe-to-extreme drought events (SPEI less than  $-1.5$ ; Figure S5). Regarding the 2018-like drought events in central Europe (Figure 6), all seven climate model simulations show a frequency similar to the one derived from observations in the historical period (1976–2005). Projections for the next decades (2006–2100) show a remarkable increase in the frequency of occurrence of 2018-like drought events (considering both the 6-month period from March to August and the summer months). All seven model simulations are coherent and consistent in this projected increase, which can be better evaluated through the estimated nonstationary intensity functions (see section 2) describing the frequency of occurrence of these large-scale drought events (Figure 6). The frequency of occurrence also reveals how these events could become the norm (see section 2) as early as 2043 (Figure 6). Three model runs show that these droughts will become the norm 13–23 years after global mean warming reaching  $3^{\circ}$  (Table S1), while in other two model runs, this will happen exactly when  $3^{\circ}$  of global mean

Comment citer ce document :

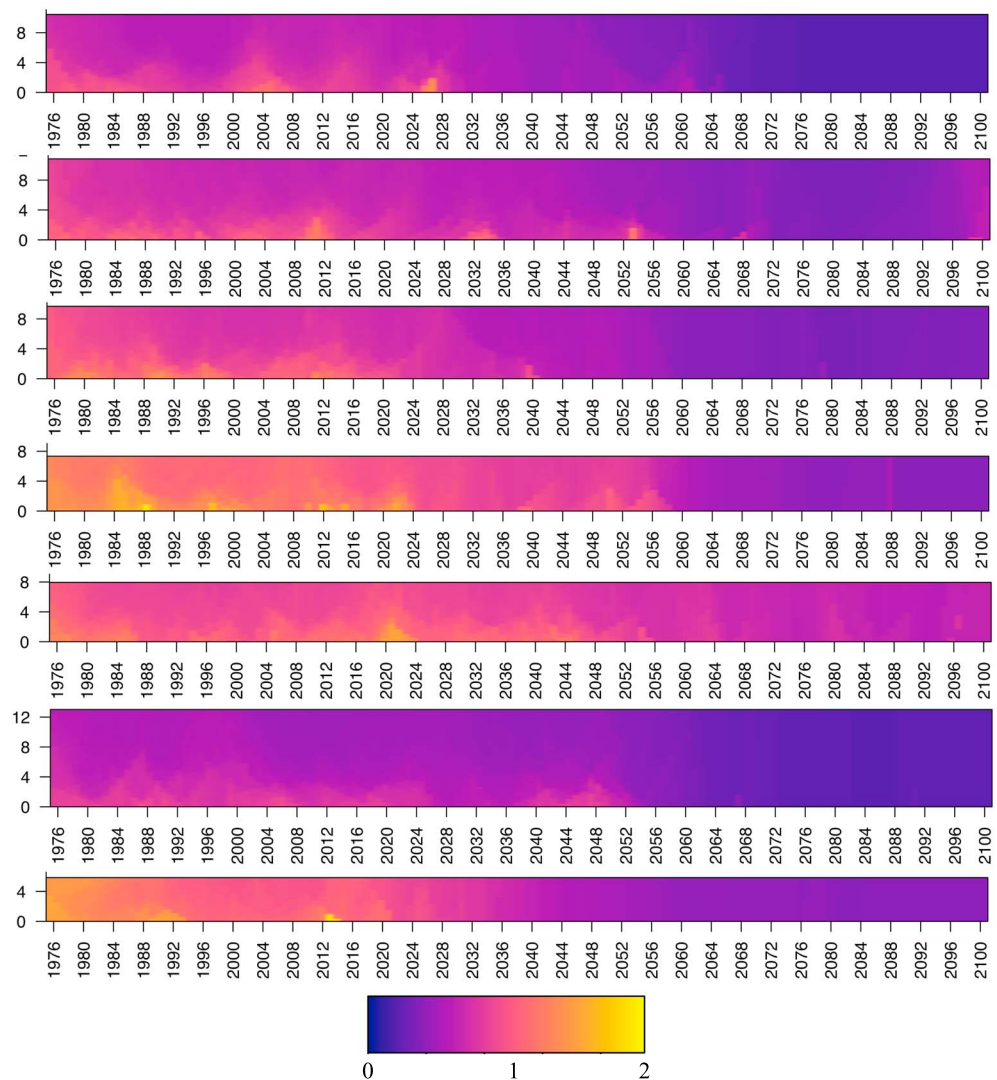


**Figure 7.** Estimated spatiotemporal (time of occurrence in the x axis and spatial extent  $\times 10^5$  in the y axis) frequency of spring-to-summer anomalous wet events (Standardized Precipitation Evapotranspiration Index  $> 1.5$ ) in southern Europe as identified in the climate model simulations from 1976 to 2100 under the high-end emission scenario RCP8.5. Values in the frequency legend are  $\times 10^{-2}$ .

warming will be reached. Only two model runs show these events being the norm already 1–6 years after having reached  $2^\circ$  of global mean warming (Table S1).

To better understand the projected drought events in central Europe as well as the uniqueness of the 2018 one, concurrent very warm and dry springs and very warm and dry summers are analyzed in the model projections (as done for the observational period and the paleoclimate reconstructions). Only a few events like the 2018 one can be identified (Figure S6). This lack of 2018-like concurrent event is mainly due to projected changes in spring precipitation regimes that reduce the frequency of as dry as 2018 conditions. Therefore, future drought events in central Europe will be mainly associated with extreme summer conditions and very warm springs.

Despite models' ability to reproduce drought events in central Europe during the historical simulations (1976–2005; Figure 6), the 2018 water seesaw (with concurrent drought and anomalous wet conditions over Europe) is reproduced only twice in two realizations, that is, in 4 years out of 875 simulated years. Furthermore, model simulations reproduce large-scale wetter conditions, such as those observed in southern Europe in 2018, very rarely. Projections show a decrease in the frequency of occurrence and spatial extension of anomalous wet conditions over those regions (Figure 7), with all model simulations pointing to

Comment citer ce document :

almost no events by mid-21st century (already by 2030s in a couple of simulations). These results imply the exceptionality of the 2018 compensation, which is not likely to occur again in the future.

#### 4. Discussion

The 2018 drought had severe impacts in a number of socioeconomic sectors (beAWARE news, 2018; WMO news, 2018), for example, higher than usual death rates among elderly people, difficulties in power plant cooling, stability issues in The Netherlands' dike system due to lack of freshwater, extremely low river levels with negative impact on the transport sector, and industries dependent on water way transport, forest fires, and notably serious impacts on agriculture. Although official production and yield estimates are not yet available, preliminary wheat production estimates (Eurostat, 2018) in the main affected countries report losses from  $-9\%$  to  $-50\%$  with respect to the mean of the previous 5 years. Barley production dropped by  $-1\%$  to  $-27\%$ . In Germany, a maize production reduction of  $-25\%$  has been reported (Eurostat, 2018). Drought also heavily affected pasture (generally not irrigated) with detrimental effects on the livestock/dairy sector. However, the positive effects of Europe's 2018 water seesaw were manifest in favorable conditions in southern Europe. Preliminary wheat production estimates report an increase of  $19\%$  in Spain and Portugal and  $24\%$  in Romania. Thus, market cooperation across the European Union could, in this instance, act as a form of adaptation to the climatic extremes experienced preventing higher volatility and price spikes.

Observations and paleoclimate reconstructions have shown the uniqueness of the 2018 event, characterized by concurrent seasonal anomalies in spring/summer temperature and precipitation. It is worth to point out that the exceptionally warm spring of 2018 turned a severe drought into an extreme drought, while it is virtually certain that the Northern Hemisphere heat events in 2018 have been caused by human-induced climate change (Vogel et al., 2019).

In the future projections, similar drought conditions in central Europe will become a common occurrence, but the 2018 event will remain unique in terms of concurrent spring and summer climate anomalies. Drought events will indeed be mainly associated with extreme temperature conditions (both in spring and summer) and very dry summer. Disentangling and quantifying the effects of mean warming conditions and atmospheric dynamics on the identified future drought events is not straightforward and requires dedicated analysis. However, an idealized experiment, obtained by rederiving the SPEI-6 from March to August (during the identified drought events) considering only the temperature component due to the mean warming (while keeping unchanged all the other factors), points to a time-dependent response. Up to a certain degree of warming (e.g., more than  $3^\circ$  for the first model simulation), the atmospheric dynamics seems to act by enhancing the mean temperature warming effects in the drought conditions. Afterward, a change in this mechanism seems to appear pointing to modified drought dynamics. Dedicated in-depth analyses are of course needed to better understand these changes in very high warming scenarios.

The projected favorable change in the spring precipitation regime in central Europe could be seen as an opportunity for adaptation, but it also points to issues that could affect agricultural risk assessments. Crop growth models (often used in such assessments) could be indeed too positively responsive to future spring precipitation, and thus, the need of having realistic representation of heat stress and soil-atmosphere fluxes in these models is essential to avoid underestimating the impacts of future drought events.

#### 5. Conclusions

The findings of this study point to the urgent need to identify realistic adaptation pathways to minimize risks and losses induced by large-scale drought events in key and complex sectors such as the agriculture. European resilience analysis for the coming decades needs to consider the projected reduced/lack of compensation given by water seesaw. Adaptation strategies for the agricultural sector will need to address concurrent water-stress conditions throughout Europe. Negative effects of the projected increase in extremes might be only partially limited by shorter phenological cycles, new varieties, and fertilization effects of increased atmospheric  $\text{CO}_2$  concentration (Challinor et al., 2016; Kimball, 2016; Obermeier et al., 2017; Parkes et al., 2018; Rezaei, Siebert, Hging, et al., 2018; Trnka et al., 2011). Crops, such as maize, could be more affected by projected increases in severe drought events (Webber et al., 2018; Zampieri et al., 2019), and as seen in 2018, the livestock sector will also be negatively impacted due to the lack of fodder crops. Besides the local impacts, it will be important to define strategies to limit the propagating effects of economic

Comment citer ce document :

shocks induced by these extremes at the European level. While market forces can play a role in mitigating the adverse effects of extreme events (e.g., global cereal prices have stabilized after the summer peak in 2018, thanks to good forecasts for wheat production in the United States and Russia; European Commission, 2018) balancing higher than expected yields from one set of European countries against losses elsewhere may not be a viable option in the future. The results presented here show that the push and pull of droughts in one region and the absence of water stress elsewhere do translate into crop yield differentials, but they also show that such water seesaw conditions are rare, and going to get rarer still, while drought occurrence will increase. Furthermore, global concurrent climate extremes must be taken into account for robust risk assessments (Toreti, Cronie, et al., 2019).

Climate change adaptation strategies for agriculture in Europe cannot count on recurrent water seesaws. It may have taken more than 500 years to reach the concurrent extreme conditions experienced in 2018, but the next 50 years will see similar conditions replicated many times over. 2018 should serve as a warning call.

### Acknowledgments

We thank L. Panarello for his support with some of the Figures and K. Wyser for useful HELIX documentation. J. Luterbacher acknowledges the DAAD (German Academic Exchange Service) project "The Mediterranean Hot-Spot: Challenges and Responses in a Changing Environment". MarsMet data can be retrieved at <http://agri4cast.jrc.ec.europa.eu/DataPortal/Index.aspx>. Paleoclimate data are available at <https://www.ncdc.noaa.gov/data-access/paleoclimatology-data/datasets/climate-reconstruction>. The SPEI data derived with HELIX projections can be downloaded at <http://data.europa.eu/89h/jrc-climate-spei-drought-helix-ec-earth-1975-2100>, while the raw HELIX projections can be requested by contacting the HELIX Project Manager <https://helixclimate.eu/>.

### References

- Allen, R. G., Pereira, L. S., Raes, D., & Smith, M. (1998). Crop evapotranspiration—Guidelines for computing crop water requirements. FAO Irrigation and drainage paper 56.
- Asseng, S., Ewert, F., Martre, P., Rötter, R. P., Lobell, D. B., Cammarano, D., et al. (2014). Rising temperatures reduce global wheat production. *Nature Climate Change*, 5, 143.
- Ayazagüena, B., Barriopedro, D., Garrido-Perez, J. M., Abalos, M., de la Camara, A., Garcia-Herrera, R., et al. (2018). Stratospheric connection to the abrupt end of the 2016/2017 Iberian drought. *Geophysical Research Letters*, 45, 12,639–12,646. <https://doi.org/10.1029/2018GL079802>
- beAWARE news (2018). Extreme weather events in the summer of 2018 in Europe. H2020-beAWARE project <https://beaware-project.eu>
- Berckmans, J., Woollings, T., Demory, M.-E., Vidale, P.-L., & Roberts, M. (2013). Atmospheric blocking in a high resolution climate model: influences of mean state, orography and eddy forcing. *Atmospheric Science Letters*, 14, 34–40.
- Briffa, K. R., van der Schrier, G., & Jones, P. D. (2009). Wet and dry summers in Europe since 1750: evidence of increasing drought. *International Journal of Climatology*, 29, 1894–1905.
- Brunner, L., Hegerl, G. C., & Steiner, A. K. (2017). Connecting atmospheric blocking to European temperature extremes in spring. *Journal of Climate*, 30, 585–594.
- Brunner, L., Schaller, N., Anstey, J., Sillmann, J., & Steiner, A. K. (2018). Dependence of present and future European temperature extremes on the location of atmospheric blocking. *Geophysical Research Letters*, 45, 6311–6320. <https://doi.org/10.1029/2018GL077837>
- Burke, E. J., Perry, R. H. J., & Brown, S. J. (2010). An extreme value analysis of UK drought and projections of change in the future. *Journal of Hydrology*, 388, 131–143.
- Challinor, A. J., Koehler, A. K., Ramirez-Villegas, J., Whitfield, S., & Das, B. (2016). Current warming will reduce yields unless maize breeding and seed systems adapt immediately. *Nature Climate Change*, 6, 954–958.
- Ciais, P., Reichstein, M., Viovy, N., Granier, A., Ogée, J., Allard, V., et al. (2005). Europe-wide reduction in primary productivity caused by the heat and drought in 2003. *Nature*, 437, 529–533.
- Dawson, A., & Palmer, T. N. (2015). Simulating weather regimes: Impact of model resolution and stochastic parameterization. *Climate Dynamics*, 44, 2177–2193.
- Dee, D. P., Uppala, S. M., Simmons, A. J., Berrisford, P., Poli, P., Kobayashi, S., et al. (2011). The ERA-Interim reanalysis: Configuration and performance of the data assimilation system. *Quarterly Journal of the Royal Meteorological Society*, 137, 553–597.
- Deryng, D., Conway, D., Ramankutty, N., Price, J., & Warren, R. (2014). Global crop yield response to extreme heat stress under multiple climate change futures. *Environmental Research Letters*, 9, 34011.
- European Commission (2018). Short-term outlook for EU agricultural markets in 2018 and 2019. DG Agriculture and Rural Development, Short-term outlook 22.
- Eurostat (2018). [ec.europa.eu/eurostat](http://ec.europa.eu/eurostat).
- Fink, A. H., Brücher, T., Krüger, A., Leckebusch, G. C., Pinto, J. G., & Ulbrich, U. (2004). The 2003 European summer heatwaves and drought synoptic diagnosis and impacts. *Weather*, 59, 209–216.
- Fontana, G., Toreti, A., Ceglar, A., & De Sanctis, G. (2015). Early heat waves over Italy and their impacts on durum wheat yields. *Natural Hazards and Earth System Sciences*, 15, 1631–1637.
- Garcia-Herrera, R., Diaz, J., Trigo, R. M., Luterbacher, J., & Fischer, E. (2010). A review of the European summer heat wave of 2003. *Critical Reviews in Environmental Science and Technology*, 40, 267–306.
- Gray, S. B., & Brady, S. M. (2016). Plant developmental responses to climate change. *Developmental Biology*, 419, 64–77.
- Hazeleger, W., Wang, X., Severijns, C., Ștefănescu, S., Bintanja, R., Sterl, A., et al. (2012). Ec-Earth v2.2: Description and validation of a new seamless earth system prediction model. *Climate Dynamics*, 39(11), 2611–2629.
- Kimball, B. A. (2016). Crop responses to elevated CO<sub>2</sub> and interactions with H<sub>2</sub>O, N, and temperature. *Current Opinion in Plant Biology*, 31, 36–43.
- Lesk, C., Rowhani, P., & Ramankutty, N. (2016). Influence of extreme weather disasters on global crop production. *Nature*, 529, 84.
- Lobell, D. B., & Gourdji, S. M. (2012). The influence of climate change on global crop productivity. *Plant Physiology*, 160, 1686–1697.
- Luterbacher, J., Dietrich, D., Xoplaki, E., Grosjean, M., & Wanner, H. (2004). European seasonal and annual temperature variability, trends, and extremes since 1500. *Science*, 303, 1499–1503.
- Miralles, D. G., Teuling, A. J., van Heerwaarden, C. C., & Vilà-Guerau de Arellano, J. (2014). Mega-heatwave temperatures due to combined soil desiccation and atmospheric heat accumulation. *Nature Geoscience*, 7, 345–349.
- Moradi, M. M., Cronie, O., Rubak, E., Lachize-Rey, R., Mateu, J., & Baddeley, A. (2019). Resample-smoothing of voronoi intensity estimators. *Statistics and Computing*. <https://doi.org/10.1007/s11222-018-09850-0>
- Naumann, G., Alfieri, L., Wyser, K., Mentaschi, L., Betts, R. A., Carrao, H., et al. (2018). Global changes in drought conditions under different levels of warming. *Geophysical Research Letters*, 45, 3285–3296. <https://doi.org/10.1002/2017GL076521>

Comment citer ce document :

Toreti, A. (Auteur de correspondance), Belward, A., PerezDominguez, I., Naumann, G., Luterbacher, J., Cronie, O., Seguin, L., Manfron, G., Lopez-Lozano, R., Baruth, B., Berg, M. v. d., Dentener, F., Ceglar, A., Chatzopoulos, T., Zampieri, M. (2019). The Exceptional 2018 European Water Seesaw Calls for Action on Adaptation. *Earth's Future*, 12 p. . DOI : 10.1029/2019EF001170



- Obermeier, W. A., Lehnert, L. W., Kammann, C. I., Müller, C., Luterbacher, J., Erbs, M., et al. (2017). Reduced CO<sub>2</sub> fertilization in temperate C<sub>3</sub> grasslands towards more extreme weather conditions. *Nature Climate Change*, 7, 137–141.
- Orth, R., Vogel, M. M., Luterbacher, J., Pfister, C., & Seneviratne, S. I. (2016a). Did European temperatures in 1540 exceed present-day records? *Environmental Research Letters*, 11, 114021.
- Orth, R., Zscheischler, J., & Seneviratne, S. I. (2016b). Record dry summer in 2015 challenges precipitation projections in central Europe. *Scientific Reports*, 6, 28334.
- Parkes, B., Sultan, B., & Ciais, P. (2018). The impact of future climate change and potential adaptation methods on maize yields in west Africa. *Climatic Change*, 151, 205–217.
- Pauling, A., Luterbacher, J., Casty, C., & Wanner, H. (2006). Five hundred years of gridded high-resolution precipitation reconstructions over Europe and the connection to large-scale circulation. *Climate Dynamics*, 26, 387–405.
- Perez-Cruz, F. (2008). Kullback-Leibler divergence estimation of continuous distributions. In *2008 IEEE international symposium on information theory*, pp. 1666–1670.
- Pfister, C. (2016). The black swan of 1540: Aspects of a European megadrought. In K. Leggewie, & F. Mauelshagen (Eds.), *Climatic change and cultural transition in Europe* (pp. 156–196). Boston: Leiden Brill.
- Porter, J. R., & Semenov, M. A. (2005). Crop responses to climatic variation. *Philosophical Transactions of the Royal Society B: Biological Sciences*, 360, 2021–2035.
- Rezaei, E. E., Siebert, S., Hüging, H., & Ewert, F. (2018). Climate change effect on wheat phenology depends on cultivar change. *Scientific Report*, 8, 4891.
- Rezaei, E. E., Siebert, S., Manderscheid, R., Müller, J., Mahrookashani, A., Ehrenpfordt, B., et al. (2018). Quantifying the response of wheat yields to heat stress: The role of the experimental setup. *Field Crops Research*, 217, 93–103.
- Spinoni, J., Naumann, G., Vogt, J. V., & Barbosa, P. (2015). The biggest drought events in Europe from 1950 to 2012. *Journal of Hydrology*, 3, 509–524.
- Stefanon, M., D'Andrea, F., & Drobinski, P. (2012). Heatwave classification over Europe and the Mediterranean region. *Environmental Research Letters*, 7, 14023.
- Toreti, A., Bassu, S., Ceglar, A., & Zampieri, M. (2019). Climate change and crop yields. In P. Ferranti, J. R. Anderson, & E. M. Berry (Eds.), *Encyclopedia of food security and sustainability* (Vol. 1, pp. 223–227). Cambridge: Elsevier.
- Toreti, O., Cronie, A., & Zampieri, M. (2019). Concurrent climate extremes in the key wheat producing regions of the world. *Scientific Reports*, 9, 5493.
- Toreti, A., Maiorano, A., De Sanctis, G., Webber, H., Ruane, A. C., Fumagalli, D., et al. (2019). Using reanalysis in crop monitoring and forecasting systems. *Agricultural Systems*, 168, 144–153.
- Trnka, M., Olesen, J. E., Kersebaum, K. C., Skjelvag, A. O., Eitzinger, J., Seguin, B., et al. (2011). Agroclimatic conditions in Europe under climate change. *Global Change Biology*, 17, 2298–2318.
- Verger, A., Baret, F., & Weiss, M. (2014). Near real-time vegetation monitoring at global scale. *IEEE Journal of Selected Topics in Applied Earth Observations and Remote Sensing*, 7, 3473–3481.
- Vicente-Serrano, S. M., Beguera, S., & Lopez-Moreno, J. I. (2010). A multiscalar drought index sensitive to global warming: The standardized precipitation evapotranspiration index. *Journal of Climate*, 23, 1696–1718.
- Vogel, M. M., Zscheischler, J., Wartenburger, R., Dee, D., & Seneviratne, S. I. (2019). Concurrent 2018 hot extremes across Northern Hemisphere due to human-induced climate change. *Earth's Future*. <https://doi.org/10.1029/2019EF001189>
- WMO news (2018). July sees extreme weather with high impacts. <https://public.wmo.int>
- Webber, H., Ewert, F., Olesen, J. E., Müller, C., Fronzek, S., Ruane, A. C., et al. (2018). Diverging importance of drought stress for maize and winter wheat in Europe. *Nature Communications*, 9, 4249.
- Wetter, O., Pfister, C., Werner, J. P., Zorita, E., Wagner, S., Seneviratne, S. I., et al. (2014). The year-long unprecedented European heat and drought of 1540—A worst case. *Climatic Change*, 125, 349–363.
- Wyser, K., Strandberg, G., Caesar, J., & Gohar, L. (2017). Documentation of changes in climate variability and extremes simulated by the HELIX AGCMs at the 3 SWLs and comparison in equivalent SST/SIC low-resolution CMIP5 projections. Helix-deliverable D3.1.
- Zampieri, M., Ceglar, A., Dentener, F., Dosio, A., Naumann, G., van den Berg, M., & Toreti, A. (2019). When will current climate extremes affecting maize production become normal? *Earth's Future*, 7, 113–122.
- Zampieri, M., Ceglar, A., Dentener, F., & Toreti, A. (2017). Wheat yield loss attributable to heat waves, drought and water excess at the global, national and subnational scales. *Environmental Research Letters*, 12, 64008.
- Zampieri, M., D'Andrea, F., Vautard, R., Ciais, P., de Noblet-Ducoudré, N., & Yiou, P. (2009). Hot European summers and the role of soil moisture in the propagation of Mediterranean drought. *Journal of Climate*, 22, 4747–4758.
- Zhao, C., Liu, B., Piao, S., Wang, X., Lobell, D. B., Huang, Y., et al. (2017). Temperature increase reduces global yields of major crops in four independent estimates. *Proceedings of the National Academy of Sciences*, 114(35), 9326–9331.